nature reviews methods primers

https://doi.org/10.1038/s43586-023-00220-3

Primer

Check for updates

# Triboelectric nanogenerators

Tinghai Cheng[1,2,4], Jiajia Shao[1,2,4] & Zhong Lin Wang[1,3]

## Abstract

By combining the effects of contact electrification and electrostatic induction, triboelectric nanogenerators (TENGs) can effectively convert mechanical energy into electric power or signals. Over the past decade, TENG development has progressed rapidly, from fundamental scientific understanding to advanced technologies and applications. This Primer gives a brief overview of TENGs, including the mechanisms of contact electrification and electrodynamics, applications, future opportunities and limitations. As an interdisciplinary field, advances are expected in both theoretical and experimental aspects of TENGs. For example, technologies based on Maxwell's equations for a mechano-driven, slow-moving system can be coupled with a theoretical understanding of physical laws and concepts. From this, general simulation models can be established and corresponding experiments designed to optimize TENGs for a range of applications.

## Sections



[1]Beijing Institute of Nanoenergy and Nanosystems, Chinese Academy of Sciences, Beijing, P. R. China. [2]School of Nanoscience and Technology, University of Chinese Academy of Sciences, Beijing, P. R. China. [3]School of Materials Science and Engineering, Georgia Institute of Technology, Atlanta, GA, USA. [4]These authors contributed equally: Tinghai Cheng, Jiajia Shao. e-mail: zlwang@gatech.edu

## Introduction

The triboelectric nanogenerator (TENG) was invented in 2012 (ref. 1). Coupling the effects of contact electrification and electrostatic induction, TENGs effectively convert mechanical energy into electric power[1–3] and can be used to make self-powered sensors and small electronics. The triboelectric effect is a type of contact electrification, where two materials become electrically charged after being separated from physical contact[2,3]. During contact electrification, charge moves by electron transfer, the direction of which depends on the materials involved. Maxwell's displacement current acts as the driving force. TENGs are most effective for converting irregular, low-frequency and low-amplitude mechanical energy into electric power, making them ideal for harvesting energy from the living environment. As energy harvesting devices, TENGs integrate multiple disciplines, including materials science, chemistry, physics, electrical engineering, medicine and more[4,5].

TENGs have been widely applied in practice, primarily in micro/nano-energy harvesting[6,7], self-powered sensors/systems[8,9], blue energy harvesting[10,11], high-voltage sources[12,13] and liquid–solid interface probes[14,15]. This Primer systematically discusses the fundamental science and advanced technologies of TENGs by examining how the triboelectric charges are created, how the electrical charges flow and how the electric current is used for advanced technologies. Before looking at these topics in detail, the theoretical background is introduced.

### Physical picture and fundamental science

**Physics of contact electrification.** An overview of the physical basis of TENGs is given in Fig. 1. A typical TENG comprises an electrode and dielectric material. With an external mechanical force, triboelectric charges are created on the contacting surfaces, and the charge density increases and saturates after several generation cycles. The triboelectric charges eventually distribute uniformly on the contacting surfaces, with a similar magnitude but opposite polarity, proved through theoretical and experimental evidence[16–20]. The triboelectric charges, also known as electrostatic charges, belong to non-moveable surface charges. There are two main categories of charges in a TENG device: triboelectric charges distributed in the dielectric material, which cannot freely move; and freely movable charges, which are induced and distributed on the electrode surface. How the triboelectric charges are generated depends on the mechanism of contact electrification and there has been debate over whether the mechanism is based on electron transfer, ion transfer or materials-species transfer. Through hard work, it has been proven that contact electrification between two solids is dominated, if not exclusively, by electron transfer[1,3,20]. An overlapped electron cloud model is demonstrated in Fig. 1B to explain contact electrification and charge transfer between two atoms as a general case. Electron transfer occurs due to the strongly overlapped electron cloud between two contacting atoms or molecules. This model is regarded as a universal model for understanding contact electrification between arbitrary contacting surfaces of dielectric materials. The model has been verified by experiments and can be extended to liquid–solid, liquid–liquid, gas–solid and gas–liquid interactions. Commonly, the electric transition model is referred to as the Wang transition for contact electrification[3].

**Medium polarization and the displacement current.** The created triboelectric charges and induced charges generate an electric field, which polarizes the dielectric material. Polarization of the dielectric material produces a second electric field that contributes to the total electric field[21–26]. How free charges are distributed on the electrodes is influenced by the total electric field and polarization. Each electrode has a different potential, which drives electron flow to decrease the

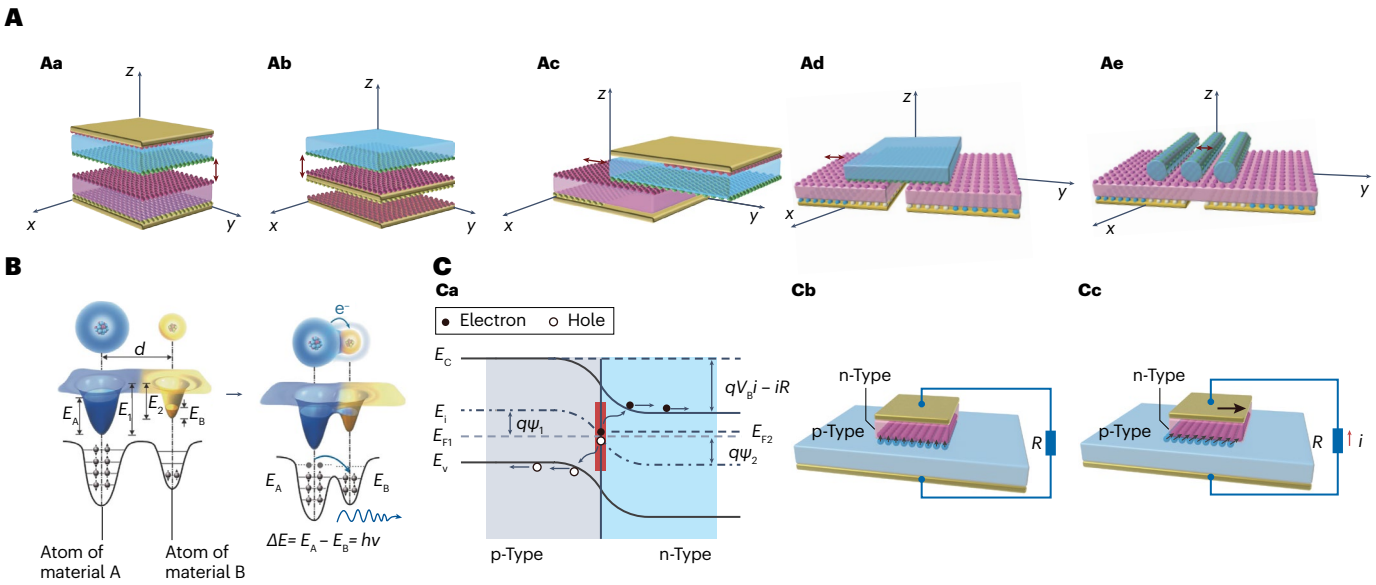


**Fig. 1 | Physical basis of TENGs. A**, Five basic models of triboelectric nanogenerators (TENGs): contact separation model (panel **Aa**), single-electrode model (panel **Ab**), lateral sliding model (panel **Ac**), freestanding model (panel **Ad**) and rolling model (panel **Ae**). Note that the dielectric layer material is represented by the light blue cuboid and the metal electrode by the golden colour. **B**, The electron cloud and potential energy well model. $E_A$ and $E_B$ represent the occupied energy levels of electrons. **C**, Energy band diagrams and the space charge distribution (panel **Ca**) as well as the connected circuit of a direct current nanogenerator (panels **Cb** and **Cc**). $E_F$ represents the Fermi level, $E_V$ the top of the valence band, $E_C$ the bottom of the conduction band, $E_i$ the intrinsic energy level, $V_B$ the built-in potential or the chemical potential difference, $q\psi$ the work function, and p-type and n-type refer to semiconductor materials. Part **A** adapted with permission from ref. 18, Elsevier. Part **B** adapted with permission from ref. 3, Wiley.

potential difference when the two electrodes are connected. As a result, an electric current is generated in the external circuit of the TENG.

The term $\boldsymbol{P_s}$ is used to describe both the polarization caused by pre-existing electrostatic charges on the media and movement driven by external mechanical excitation that results in polarization. The $\boldsymbol{P_s}$ term is referred to as mechano-induced polarization owing to the variation of media distribution in space[27–31]. Meanwhile, the electric displacement vector ($\boldsymbol{D}$) is modified to[32,33]:

$$D = \varepsilon_0 E + P + P_s = \varepsilon E + P_s = D' + P_s \tag{1}$$

where $\boldsymbol{E}$ represents the total electric field inside the dielectric media, including the portion generated by both the external electric field and media polarization, whereas $\boldsymbol{P}$ is the dielectric polarization caused by an external electric field. $\varepsilon_0$ is the permittivity vacuum, $\varepsilon$ represents the relative dielectric constant and $\boldsymbol{D'}$ is the traditional definition of the electric displacement vector. The additional term $\boldsymbol{P_s}$ estimates the coupling effects of media polarization and energy conversion due to mechanical excitation[27–31]. Redefinition of the electric displacement vector, $\boldsymbol{D}$, means the displacement current in either the dielectric medium or the vacuum should be redefined. Subsequently, the total displacement current ($\boldsymbol{J_D}$) is redefined as:

$$J_D = \frac{\partial D'}{\partial t} + \frac{\partial P_s}{\partial t} = \varepsilon \frac{\partial E}{\partial t} + \frac{\partial P_s}{\partial t} \tag{2}$$

where $\varepsilon \frac{\partial E}{\partial t}$ represents the displacement current responsible for electromagnetic waves travelling at the speed of light in vacuum[27,28]. $\frac{\partial P_s}{\partial t}$ is the time-dependent polarization for non-electric field effects, which is responsible for energy conversion and sensors[27,28], widely known as the Wang term[1,3]. The electromagnetic energy distributed in $\frac{\partial P_s}{\partial t}$ comes from an external mechanical energy source travelling at a small speed, slower than the speed of light in most cases. Importantly, Eq. (2) proves that Maxwell's displacement current is the driving force of TENGs.

Using the newly defined $\boldsymbol{D}$, the classical Maxwell's equations are[27,28]:

$$\nabla \cdot D' = \rho_f - \nabla \cdot P_S \tag{3}$$

$$\nabla \cdot B = 0 \tag{4}$$

$$\nabla \times E = -\frac{\partial}{\partial t} B \tag{5}$$

$$\nabla \times H = J_f + \frac{\partial}{\partial t} D' + \frac{\partial}{\partial t} P_S \tag{6}$$

where $\rho_f$ represents the free charge density and $\boldsymbol{J_f}$ is the free current density; $\boldsymbol{B}$ and $\boldsymbol{H}$ are the magnetic field and magnetizing field, respectively. Note that the above set of four equations are self-consistent and satisfy the law of conservation of charges[27,28].

**Maxwell's equations for a mechano-driven slow-moving media system.** For a general TENG device, the charged dielectric medium can move with an arbitrary velocity distribution under mechanical excitation. This external mechanical energy source deforms the dielectric materials. Recently, experimental results have demonstrated that the electromagnetic radiation generated by a TENG occurs due to the relative media movement[34–36]. If a TENG operates at an extremely high frequency — such as hundreds of megahertz — an alternating current (AC) oscillating current will be produced. The corresponding high-frequency electromagnetic field between the electrodes will unavoidably radiate electromagnetic waves[34–36]. From the experimental evidence, the TENG device can be considered a special kind of mechanical antenna, which connects electromagnetic wave propagation and energy conversion.

For a medium that has a time-dependent volume, shape and boundary, moving at an inhomogeneous velocity $\boldsymbol{v}(\boldsymbol{r}, t)$ with an arbitrary trajectory distribution, the Maxwell's equations for a mechano-driven slow-moving medium system (MEs-f-MDMS) are directly proposed[27–31]. The expanded MEs-f-MDMS are derived from the integral forms of four physical laws, which combine the mechano-electromagnetic interaction fields, enabling the complex dynamic electromagnetic phenomena of a moving medium to be revealed. A motion-generated electromagnetic field in a medium caused by the moving charged dielectric material of a TENG can be investigated by MEs-f-MDMS. Propagation in space can be described through Maxwell's equations, which both meet at the medium interface, as governed by the boundary conditions[27–31].

If the medium moves in an arbitrary low-velocity distribution, even with an inhomogeneous velocity such as variable motion, the electrodynamics inside the media are governed by[28]:

$$\nabla \cdot D' = \rho_f \tag{7}$$

$$\nabla \cdot B = 0 \tag{8}$$

$$\nabla \times (E + v_r \times B) = -\frac{\partial}{\partial t} B \tag{9}$$

$$\nabla \times (H - v_r \times D') = J_f + \rho_f v + \frac{\partial}{\partial t} D' \tag{10}$$

where $\boldsymbol{v}$ represents the moving velocity of the reference frame for the media and $\boldsymbol{v_r}$ is the relative moving velocity of the charge with respect to the moving reference frame. The $\boldsymbol{v_r}$ term drops out in two cases: if the free moveable charge and moving medium have no relative velocity; or if the free moveable charge inside the medium moves parallel to the circuit's internal path, $[v_r \times B] \cdot dL = 0$. If the mechano-driven polarization term $\boldsymbol{P_s}$ is included to describe additional polarization introduced by the media's motion with respect to the moving reference frame, Eqs. (7–10) become:

$$\nabla \cdot D' = \rho_f - \nabla \cdot P_s \tag{11}$$

$$\nabla \cdot B = 0 \tag{12}$$

$$\nabla \times (E + v_r \times B) = -\frac{\partial}{\partial t} B \tag{13}$$

$$\nabla \times [H - v_r \times (D' + P_S)] = J_f + \rho_f v + \frac{\partial}{\partial t} (D' + P_S) \tag{14}$$

The expanded Maxwell's equations are the most comprehensive governing equations, coupling the three areas of mechanics, electricity and magnetism[27,28]. The modified Maxwell's equations provide a suitable description of the fundamental science of TENGs, integrating the electromagnetic phenomenon, power generation and their interaction.

For the non-inertial system described by Eqs. (7–10), because there is an input of external energy into system, the energy of electricity and magnetism is not conserved, meaning the MEs-f-MDMS do not satisfy Lorentz covariance[27–31]. However, the electromagnetic wave within the medium $c_m$ cannot exceed the speed of light $c_0$ in a vacuum. This is due to the medium's permittivity, which causes light inside the media to be slower than $c_0$ and $\boldsymbol{v}_r \leq c_m$ (refs. 27–31). An electromagnetic wave travelling in vacuum space is governed by the classical Maxwell's equations, with a velocity of $c_0$ irrespective of whether the medium is moving. Boundary conditions require solutions of the classical and expanded Maxwell's equations to meet at the medium boundary, which can be derived from the corresponding integral form of the equations[28,33].

## Experimentation

### Conceptualization and fundamental modes

Using the displacement current as the driving force, TENGs can convert mechanical energy into electric power or signal[3,5,37]. A TENG contains at least two components: the conductive electrode and dielectric material. Common electrode materials include metals and other conductive, flexible materials. The conductive electrode acts as a free charge collector and free movable charges can flow between the two electrodes. Dielectric materials, such as PTFE and fluorinated ethylene propylene (FEP), are used to create triboelectric charges — free charges that cannot move due to the extremely low conductivity of the dielectric medium. The triboelectric charges are necessary to generate an electric field. External mechanical agitation is also required to act as an energy input source.

Many types of TENGs have been designed and constructed. They can be divided into five basic models, as illustrated in Fig. 1A: contact separation[38], single electrode[39], lateral sliding[40], freestanding[41] and rolling[42]. Each model has its own basic structure and advantages, which can be applied to a suitable corresponding circumstance. For instance, a TENG device with any configuration is neutral and can be considered a lumped element, described by a lumped parameter. The special working mechanism of a TENG means the output power is approximately proportional to the working frequency. As a result, TENGs are usually operated under low frequency, with better performance than electromagnetic generators (typically 0.1–3 Hz). In addition, as there is only one electrode in the single-electrode mode TENG, half the inductive charges distributed in the electrode can be transferred. For a freestanding mode TENG, particularly a contact separation freestanding mode TENG, the inherent capacitance is time invariant and the open circuit voltage is completely linear with moving distance. This feature makes it a linear and time-invariant device that can be used as an energy harvesting system or self-powered sensor. Figure 1B shows an overlapped electron cloud model to describe the mechanism of contact electrification and charge transfer. Another form of energy conversion device is demonstrated in Fig. 1C, referred to as a direct current (DC) model TENG. p-Type and n-type refer to semiconductor materials. This model does not belong to the five basic TENG models mentioned earlier, and is a new and special energy harvesting device. Although its fundamental mechanism is currently unknown, the high output performance of DC model TENGs presents potential for next-generation self-powered electronics and self-powered sensors.

### Materials and fabrication

Material durability also influences the output performance of a TENG. Widely used materials for TENGs include ceramics, polymers, metals and semiconductors. The process of contact electrification occurs in solid, liquid and gaseous forms. Metals, ceramics, semiconductors and polymers are examples of solid-state materials that can be used for TENGs. For liquids, water, oils, liquid metals and aqueous solutions at various pH values can be used. In general, solid–solid contact electrification is dominated by electron transfer. Both electrons and ions are transferred during liquid–solid contact electrification. Quantifying the triboelectric series of various polymers enables the surface triboelectrification of general materials to be established as a material property. The intrinsic affinity of a polymer to gain or lose electrons can be derived from the normalized triboelectric charge density. Two factors should be considered when choosing a TENG material: high charge density and high durability. High charge density determines the TENG output performance, whereas high durability enables TENGs to have greater stability and a longer service life than the conventional TENGs. The quantitative triboelectric series can be used to guide TENG applications in energy harvesting and self-powered sensing. Modifications to TENG materials can be achieved by ion sputtering, atomic deposition, electrostatic spinning and more. Fabrication methods include 3D printing and laser engraving. Preparation of a TENG is relatively straightforward, as a typical TENG contains two materials with different electronegativity that are pasted separately onto an acrylic substrate. New developments, such as bionic design and mechanical structure design, have started to be used to prepare TENGs[43].

### Equipment and measurement

The test platform contains an external excitation system, measurement equipment and a data acquisition device. The output characteristics of a TENG require a series of devices with various motion. For a TENG with linear and rotatory motion modes, a linear motor and a rotary motor are needed. TENGs have high sensitivity and are easily disturbed by the external environment, meaning it is important that the motors used have minimal interference. In addition, special movements, such as swinging or spiral movements, cannot be measured by the machine and a specialized design is needed to detect them. The high voltage, low current and high impedance characteristics of a TENG mean common instruments, such as oscilloscopes, cannot provide accurate measurements. As a result, programmable electrometers are used because they have an internal resistance of 200 TΩ and are hardly affected by the high internal resistance of a TENG. For an oscilloscope with internal resistance of 10 MΩ, if the internal resistance of the oscilloscope is equivalent to a larger internal resistance in TENG, the output value is quite different from the real value. Even with a high-impedance probe of 100 MΩ, there is still a large difference. Research has improved the output performance of TENGs exponentially and the programmable electrometer can no longer meet the demand of voltage measurements. Consequently, the high-voltage high-speed surface potentiometer is used, which can measure the voltage from several thousand volts to tens of thousands of volts. Although the test instrument can measure data, it cannot store data. Data acquisition cards can visualize and store test data using the LabVIEW program. The collected data are processed according to requirements. Development and application of TENGs to self-driven sensing have led to powerful data acquisition cards, which can directly measure and collect data in LabVIEW when combined with a step-down module.

## Results

### Theoretical modelling of TENGs

Internal rules of matter can be reflected through an established model. To clarify how the electrical charge flows and predict the output

characteristics of a TENG, three theoretical models have been constructed (Fig. 2a–c): a mathematical-physical model based on Maxwell's equations[3,18,19]; the equivalent circuit model — including the capacitor model[22,23] (Fig. 2a) and Norton's equivalent circuit model[5,24] (Fig. 2b) — based on the theory of a lumped-parameter equivalent circuit; and a universal dynamic simulation model that couples the quasi-electrostatic mode and electrical circuit model[5,24,26] (Fig. 2c). The mathematical-physical model includes 3D mathematical modelling[5,18,19] and distance-dependent electric field modelling[16,17], both of which are part of the quasi-electrostatic model[5]. Because TENGs typically work at low frequencies under the quasi-static condition, the fields generated by a TENG — such as the time-dependent electric field — change slowly. In the capacitor model, a TENG is equivalent to a series connection of a voltage source and a variable capacitor[44].

Based on the capacitor model and the relationships among the voltage, charge and separation distance ($V$–$Q$–$x$), the governing equation of the capacitor model is given by[5,44]:

$$V = -\frac{Q}{C(x)} + V_{OC}(x) \tag{15}$$

where $C(x)$ represents the TENG capacitance, $Q$ is the output charge and $V_{oc}$ is the open circuit voltage. This is a first-order ordinary differential equation, where the output charge is the dependent variable. With boundary condition $Q(t = 0) = 0$, this equation can be solved. From the time-dependent 3D mathematical model, the governing equation of the TENG can be written as[5,18]:

$$-ZA\frac{d\sigma_U}{dt} = \phi_1(x_1, y_1, z_1) - \phi_2(x_2, y_2, z_2) \tag{16}$$

where $\sigma_U(t)$ represents the transferred charge density between electrodes, $Z$ is an external electric impedance and $A$ is the contacting surface. The electrical potentials of two electrodes are expressed by $\phi_1(x_1, y_1, z_1)$ and $\phi_2(x_2, y_2, z_2)$, respectively. Equation (16) is a time-dependent differential equation, from which $\sigma_U(t)$ is obtained. Subsequently, the current, transient power, electrical energy and average power of the TENG can be calculated.

According to Norton's theorem, the capacitor model is converted into an equivalent Norton's circuit model and the TENG is represented by a time-varying current source connected in parallel to an internal impedance[5,24,26]. The time-varying displacement current calculated under a short circuit condition is the current source of a TENG. This is why it can be proved that the displacement current is the driving source of a TENG. The TENG energy harvesting system includes mechanical energy and electrical energy, coupled by the TENG transducer[5]. To accurately control and predict the energy harvesting process, an electromechanical coupling model has been constructed[2,5]. This coupling model contains both a mechanical model and an equivalent circuit model. There are three typical energy fields in the energy harvesting system: the mechanical energy field provided by external excitation, the quasi-electrostatic field created by the transfer of electrical charges distributed in the TENG and the output electrical energy extracted to the external circuit through the special power management circuit.

## Maximum output power and design rules

Making a TENG device or array output maximum power and energy involves many factors[21]. This is mainly influenced by mechanical characteristics, geometric parameters, material parameters, global motion parameters, loading conditions and physical effects such as edge effects, discharge effects and coupling effects, and ambient conditions such as humidity and temperature. The challenge in predicting maximum output power is to condense all necessary elements in the energy harvesting system. General optimization guidelines for TENGs can be determined from the optimum condition of the TENG transducer, the loading condition and how these two factors combine. Optimized capacitance and external load resistance both play a key role in improving the average output power[45]. However, clarifying the

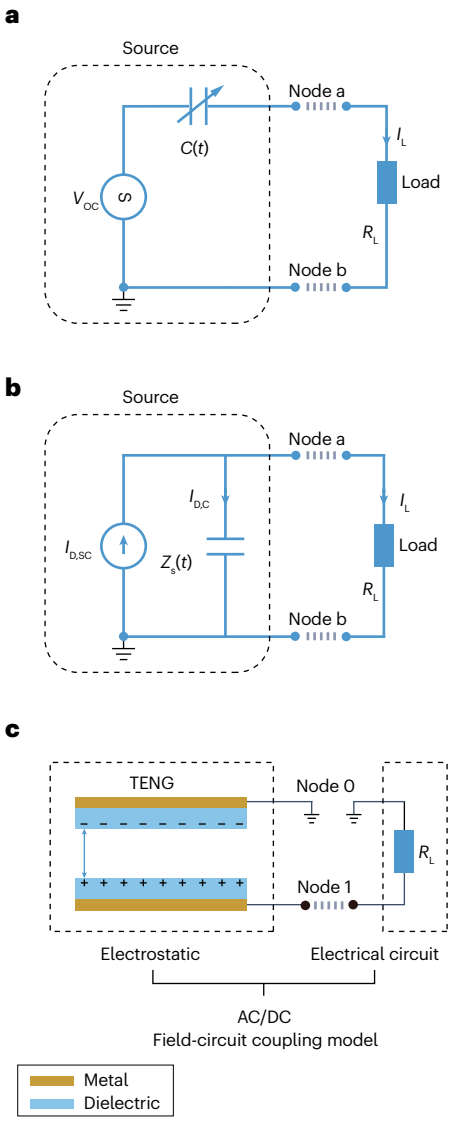


**Fig. 2 | Equivalent circuit models of TENGs. a**, Capacitance model of triboelectric nanogenerators (TENGs). **b**, Norton's equivalent circuit model. **c**, A universal dynamic simulation model, which couples the quasi-electrostatic mode and electrical circuit model together. $V_{OC}$ is the open circuit voltage, $C(t)$ the capacitance of the TENG device, $R_L$ the external connected resistor, $I_{D,SC}$ the displacement current obtained at short circuit conditions, $I_{D,C}$ the displacement current through the internal equivalent capacitor, $Z_S(t)$ the time-dependent resistor of the TENG device and $I_L$ the conduction current flowing in the external circuit. AC, alternating current; DC, direct current. Parts **b** and **c** adapted with permission from ref. 24, IOP.

optimum conditions of a TENG array is extremely different to a TENG device and often more complicated. For an array, edge effects caused by the fringing electric field need to be considered. To address this, exact adjustment of the gap distance between each TENG device is required[27]. Additionally, the mechanical excitation and external circuit condition should be considered as they can enhance the maximum output power.

### Figures of merit

Evaluating the output characteristics of TENGs with different configurations presents an issue to be solved. Figures of merit that have been proposed include the structural figure of merit ($FOM_S$)[46], material figure of merit ($FOM_M$)[46] and device figure of merit ($FOM_{device}$)[45]. These three metrics are regarded as the universal standard for TENGs. $FOM_S$ is calculated by $2(\varepsilon_0 E_m)/(\sigma^2 A x_{max})$, where $\varepsilon_0$ is the permittivity of the vacuum, $E_m$ represents the largest possible output energy per cycle, $\sigma$ is the triboelectric charge density distributed at the contacting surface, $A$ represents the contacting surface area and $x_{max}$ is the largest relative displacement between the triboelectric layers. $FOM_S$ mainly depends on structural parameters and $x_{max}$, illustrating the structural design advantages of TENGs. $FOM_M$ is related to the ability of a triboelectric material to generate triboelectric charges, equivalent to $\sigma^2$. $FOM_{device}$ is heavily reliant on the maximum power density[45], which is defined by $FOM_{device} = 0.064(\bar{v}\sigma^2)/\varepsilon_0$, where $\bar{v} = (\omega x_{max})/\pi$ represents the average speed of the external mechanical motion. Another approach is to use the practical output energy, rather than the theoretical maximum energy per cycle. The structural figure of merit ($FOM_{RS}$) under optimum resistance has also been proposed[22,28], as it is more practical and achievable compared with parameters measured under an open circuit condition. Another TENG structural figure of merit covers steady-state ($FOM_T$) operation[19,25].

## Applications

TENGs can be used across a wide range of applications, including micro/nano-energy harvesting[6,7], self-powered sensors or systems[8,9], blue energy harvesting[10,11], as a high-voltage source[12,13] and as a liquid–solid interface probe[14,15]. As a micro/nano-energy harvester, TENGs can provide a steady stream of energy for micro-miniature devices, such as electronic skin, implantable medical devices, wearable flexible electronics and more. When operating as a self-powered sensor or system, TENGs can provide health monitoring, biosensing, human–computer interaction, environmental monitoring and infrastructure security. TENG-based network units can collect low-frequency seawater movement energy, which may be used in the future for pollution-free blue energy. TENGs can also act as a high-voltage source in plasma, electrostatic spinning fibres and particle filters. In addition, when using TENGs as a liquid–solid interface probe, advances may be gained in research fields related to the electric double layer (EDL), for example electrophoresis, mechanochemistry, electrochemical storage and electrocatalysis. From microscopic energy harvesting to macroscopic high energy-density power generation, from tiny mechanical vibrations to ocean movement, the nanogenerator energy system has a solid technical foundation for integration of nano-devices and large-scale self-supply energy. This will benefit a broad spectrum of fields, including networking, health care, medicine, environmental protection, national defence security and artificial intelligence.

### Micro/nano-energy harvesting

Micro/nano energy — such as wind energy, water energy, vibration energy and human motion — is ubiquitous across the ambient environment. Micro and nanotechnologies, including TENGs, have been used to efficiently harvest and store energy from the natural environment or human motion to provide lasting, maintenance-free, self-driven energy. TENGs can be widely applied in areas such as smart traffic, smart factories and mechanical sensing[47–51] (Fig. 3a). As depicted in Fig. 3b, TENGs with various motion types such as linear[52], rotation[53], swing[54] and vibration[55] are designed and fabricated for environment energy harvesting, which provide micro-power sources for small electronic devices. Assembly and integration of basic units enables large-scale energy harvesting. However, TENGs have a high load output, which results in high voltage and low current output. As a result, existing AC output characteristics constrain the application and development of TENGs. Numerous energy modules[56] have been proposed to solve this issue. The power management components, rectifiers and energy storage components of TENGs enable suitable DC voltage output (Fig. 3c). Additionally, the rectified pulsed output can be directly used to drive electronic devices and electrochemical applications[57–59]. In Fig. 3d, various TENG-based self-powered systems are presented[60–63].

### Self-powered sensors and systems

A new generation of sensing technology is needed to keep up with the rapidly developing Internet of Things and TENGs are becoming increasingly critical in sensor technology. TENG-based sensors are passive sensors that convert measurement information into electrical signals, referred to as triboelectric sensor (TESs). In Fig. 4a, the TES uses interval arrangement electrodes to convert mechanical energy into pulsed signals via mechanical motion. The waveform information generated by a TES includes physical parameters, such as the waveform phase ($\varphi$), pulse frequency ($f$) and pulse amplitude ($A$), as depicted in Fig. 4b. Figure 4c shows how TESs can be classified according to their electrodes and form of motion. In addition, the original signals generated by a TES need to be collected by the microcontroller unit (MCU) and input into the digital to analogue converter (DAC), where the digital signal is transformed into an analogue signal and sent to the operating controller. In Fig. 4d, the TES-based self-powered system includes the self-powered sensor for signal generation, the processing circuit for converting the signal into a square wave, the MCU for calculating the number of generated pulses, the wireless transmitter module for sending command signals, the wireless signal receiver and the operating system. The physical parameters reflected by the waveform signal of TESs have different applications under specific environmental conditions. For the pulse number, a badge reel-type stretch sensor based on a grating-structured TENG is used to achieve low hysteresis and high durability[64]. For the pulse frequency, a bearing-type TENG is fabricated by 3D printing to use as an energy collector or a self-powered sensor[65]. For the waveform phase, a thin, lightweight triboelectric self-powered angle sensor with high resolution is proposed[66] to aid the sensor's integrated application. For example, a highly sensitive triboelectric self-powered angle sensor can be assembled in a medical stent that records joint flexion and extension to benefit personalized treatment. Finally, for the pulse amplitude, a lightweight, comfortable, breathable, flexible and self-powered all-nanofibre electronic skin-based TENG is proposed. This electronic skin is simple, low cost, highly sensitive (0.217 $kPa^{-1}$), comfortable and flexible[67].

### Blue energy harvesting

There is a large amount of marine energy contained in the world's oceans. Tapping into this energy source has attracted the attention of many nations[68]. Efficient energy conversion of ocean waves is limited due to its low-frequency, intermittent and random nature. TENGs are

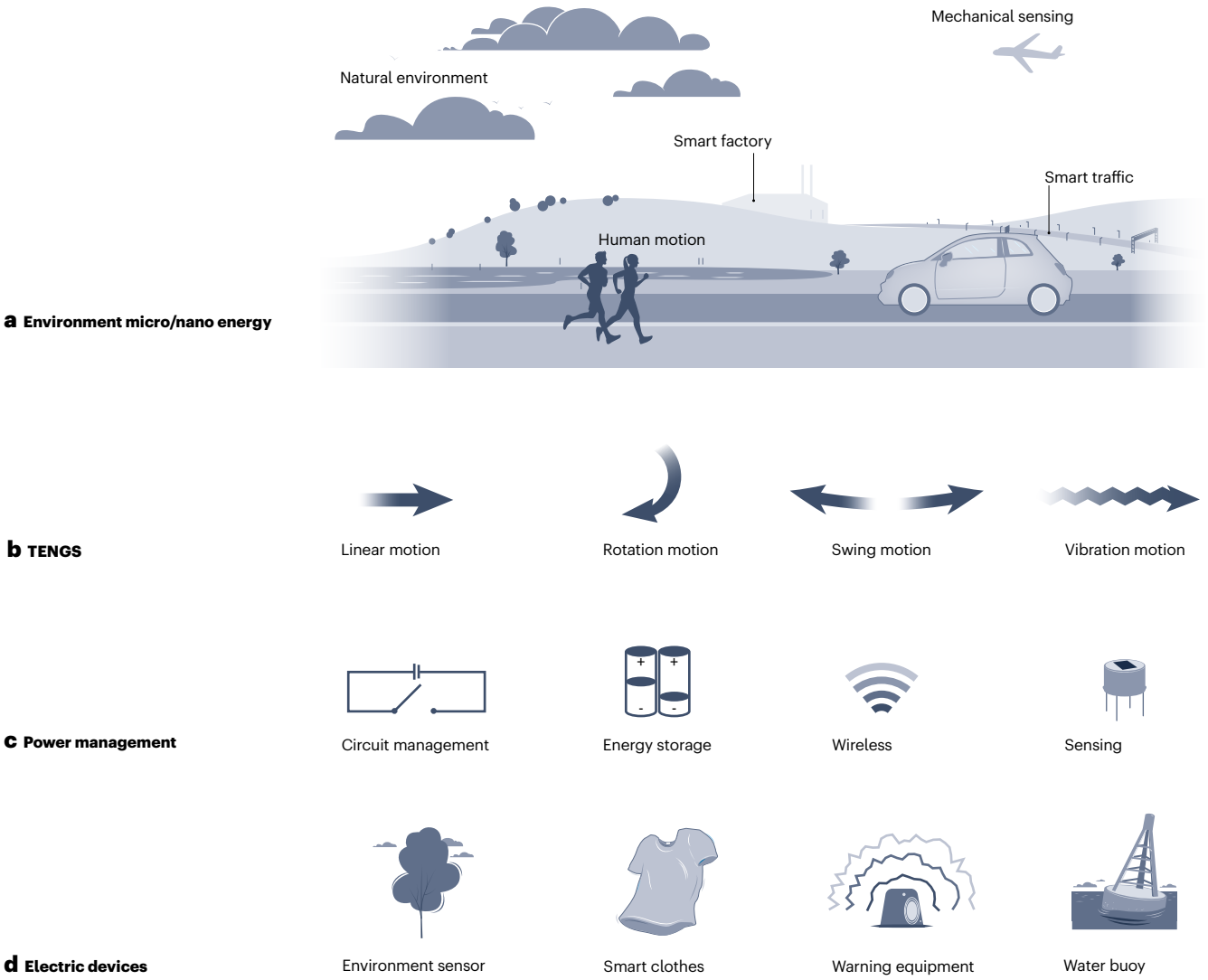


**Fig. 3 | Applications of TENGs as micro/nano-energy harvesters. a**, Scenes of micro/nano energy including the natural environment, human motion, smart traffic, smart factory and mechanical sensing. **b**, Triboelectric nanogenerator (TENG) with various motion types such as linear, rotation, swing and vibration for energy harvesting. **c**, Power management of TENGs, including circuit management, energy storage, wireless operation and sensing. **d**, TENGs for powering environment sensors, smart clothes, warning equipment and water buoys.

advantageous for harvesting blue energy as they have an extremely high conversion efficiency for low-frequency energy[43,69]. It has been proposed that TENG floating nets be used to harvest wave energy from the ocean[70], shown in Fig. 5a. In this set-up, a network structure is integrated with multiple TENG units. To improve the autonomy and robustness of the system, encapsulated multi-TENGs are constructed into a macroscopic self-assembly network for water wave energy harvesting[71] (Fig. 5b). A high-performance TENG with charge shuttling can (Fig. 5c) improve surface charge density[72]. To enhance durability, a high-efficiency swing-structure TENG can be used to collect ultra-low-frequency water wave energy[73], as shown in Fig. 5d. The internal swing structure extends the running time, increasing performance output. A power network can be achieved by connecting millions of spherical TENG components. The components can be arranged above or below the water surface to form a 3D network structure. Building a TENG network is a potential method of collecting large-scale blue energy[74]. In Fig. 5e, a self-powered smart buoy system based on TENGs is shown[62]. The output AC is converted into DC through the power management module to supply power to the control module. To achieve energy harvesting and self-powered sensing, a spherical TENG with a spring-assisted multilayer structure can be used to harvest multidirectional water wave energy (Fig. 5f). The output energy is managed by the power management module[56].

## Other applications

TENGs can be considered high-voltage power sources. Compared with traditional high-voltage power sources there are advantages to using TENG-based sources, such as improved safety, simpler structure,

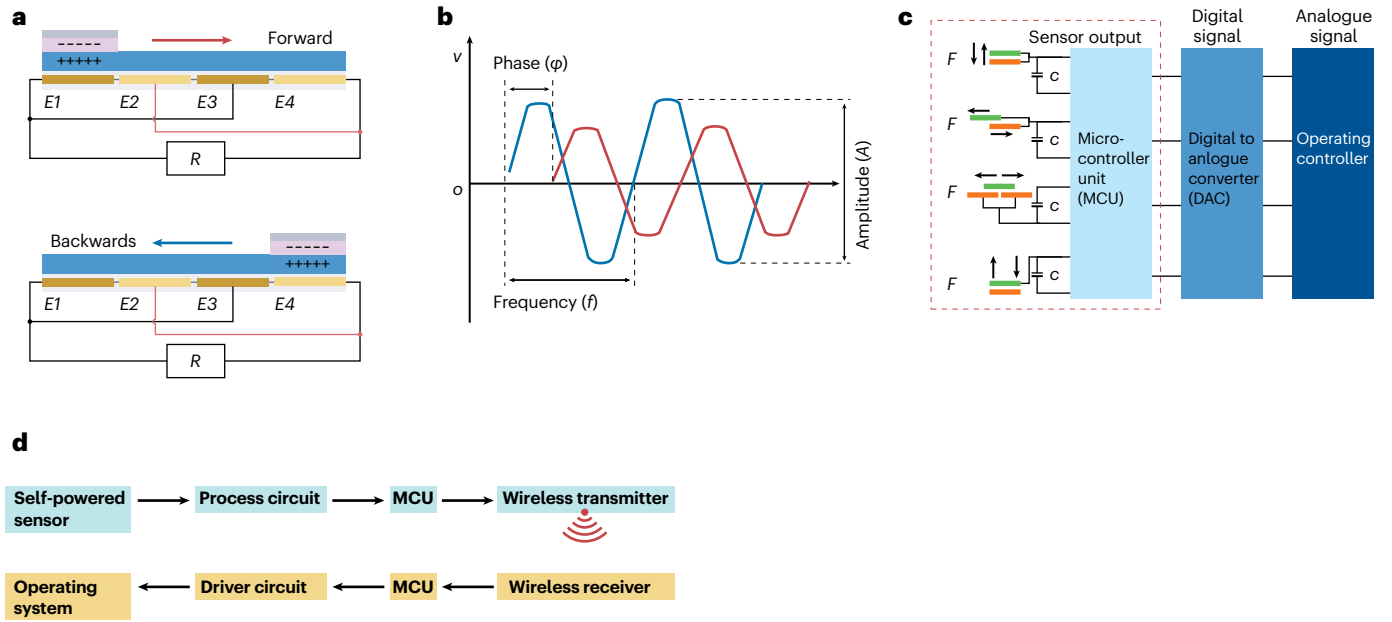


**Fig. 4 | Applications of TENGs as self-powered sensors/systems. a**, The grating-like electrode part and the slider part. **b**, Output waveform and sensing parameter labelling of a triboelectric sensor (TES). **c**, Signal processing flow of a TES with four working modes. **d**, Wireless transmission flow chart of a TES. TENG, triboelectric nanogenerator. MCU, microcontroller unit.

greater portability and being more cost-effective. By combining TENG-based high-voltage power sources and plasma sources, a triboelectric microplasma is created[12] (Fig. 6a), which is an atmospheric-pressure plasma driven by mechanical stimuli. A multilayered reusable triboelectric air filter (TAF) composed of nylon and PTFE[13] is shown in Fig. 6b. When the nylon and PTFE fabrics are rubbed together, the TAF is easily charged. After charging, the TAF has removal efficiencies of 84.7% and 96.0% for $PM_{0.5}$ and $PM_{2.5}$, respectively, demonstrating the potential of TENG-based air purification. A TENG with a charge accumulation strategy is proposed to provide a sustainable ultra-high output voltage[75]. The ultra-high voltage enables self-powered oil purification by triggering continuous electrophoresis and dielectrophoresis effects (Fig. 6c). As shown in Fig. 6d, the TENG electrodes are maintained at optimal voltage and surface charge density using the charge replenishment channel, based on a charge-dissipative mechanism. An electroadhesion system with this boosted voltage can manipulate objects[76]. For solid–solid applications, an example is shown in Fig. 6e based on atomic force microscopy, which is used to measure local surface charge densities[14]. Electrostatic induction occurs between a conductive tip and a dielectric bottom electrode. In scanning TENG, a conductive tip taps above a charged dielectric surface. Scanning TENG is a powerful tool for probing nanoscale charge transfer in contact electrification. To measure the charge transfer in a liquid–solid interface, a self-powered droplet TENG has been developed[15] (Fig. 6f). Electrons are the dominant species of charge transfer between droplets and solids, as shown by the electric signals on spatially arranged electrodes. For interface spectroscopy, the photon emission spectrum is measured during contact electrification between two solid materials[77], as shown in Fig. 6g. During this process, electrons are transferred between atoms at the interface of two materials.

## Reproducibility and data deposition

Several factors influence the reproducibility of experimental results. They can be divided into three groups: factors related to the selection of triboelectric materials[78,79], related to instrumentation and experimental methods, and related to the test environment. For theoretical calculations and simulations, repeatability is not an issue. Material selection is the first and most fundamental step. Based on the proposed figure of merit, it is well documented that the TENG output performance is strongly dependent on the triboelectric charge density. Therefore, suitable materials must be chosen for the TENG device. A quantitative triboelectric series has been constructed using a universal method involving standardized evaluation of different materials' triboelectric charge density in a controlled environment[80,81]. The triboelectric charge density, to a certain extent, demonstrates the material's capability to obtain or lose electrons after contact electrification. This provides a theoretical basis and practical reference point to design and fabricate TENGs. Once a TENG device is fabricated, its electrical output performance – such as the open circuit voltage and the short circuit current – is measured by an electrometer. The external mechanical excitation can be provided by a linear motor, with the help of a linear motor control programme and system. For self-powered sensors based on TENGs, the electrical output signals and power should be tested with relevant equipment.

Material selection and test equipment can be controlled, but external factors may also impact reproducibility. The environment temperature, humidity and electromagnetic environment all affect triboelectric charge generation, influencing the output performance[80,82]. High temperature, high humidity, pollution and strong electromagnetic interference significantly reduce the output stability performance. For theoretical simulations, there is generally good reproducibility and stability. Numerical simulations at open circuit, short circuit and loading conditions are performed with, for instance, COMSOL Multiphysics

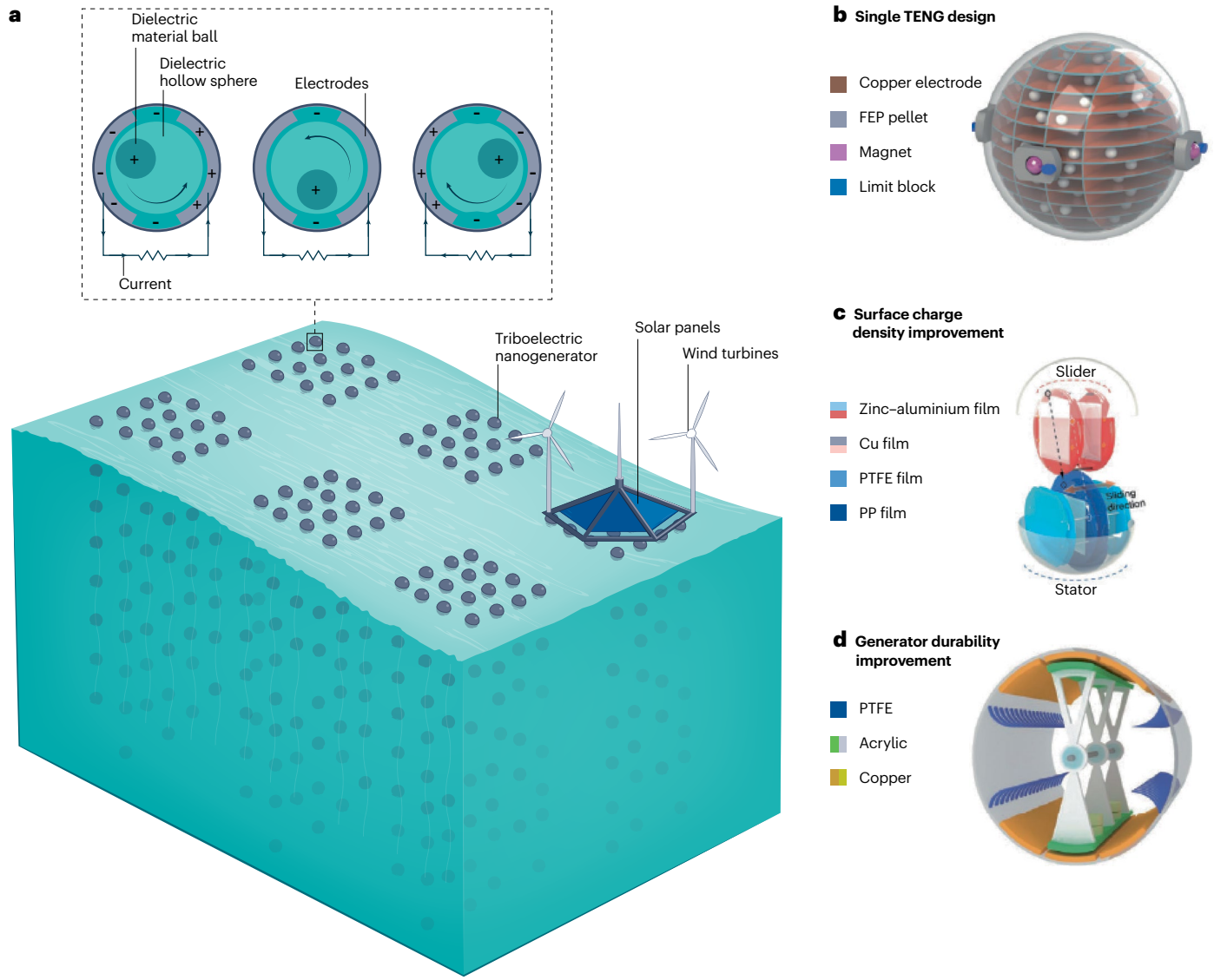


**Fig. 5 | Applications of TENGs in blue energy harvesting. a**, Triboelectric nanogenerator (TENG) for harvesting blue energy. **b**, A single TENG unit. **c**, TENG with high surface charge density. **d**, 3D structure and cross-section for the swing-structured TENG. **e**, Management and storage of a TENG for harvesting water wave energy. **f**, Water wave energy harvested by TENG for self-powered sensing. CEC, charge excitation circuit; FEP, fluorinated ethylene propylene. Part **a** reprinted from ref. 70, Springer Nature Limited. Part **b** reprinted with permission from ref. 71, Elsevier. Part **c** reprinted from ref. 72, Springer Nature Limited. Part **d** reprinted with permission from ref. 73, Wiley. Part **e** reprinted with permission from ref. 62, Elsevier. Part **f** reprinted with permission from ref. 56, RSC.

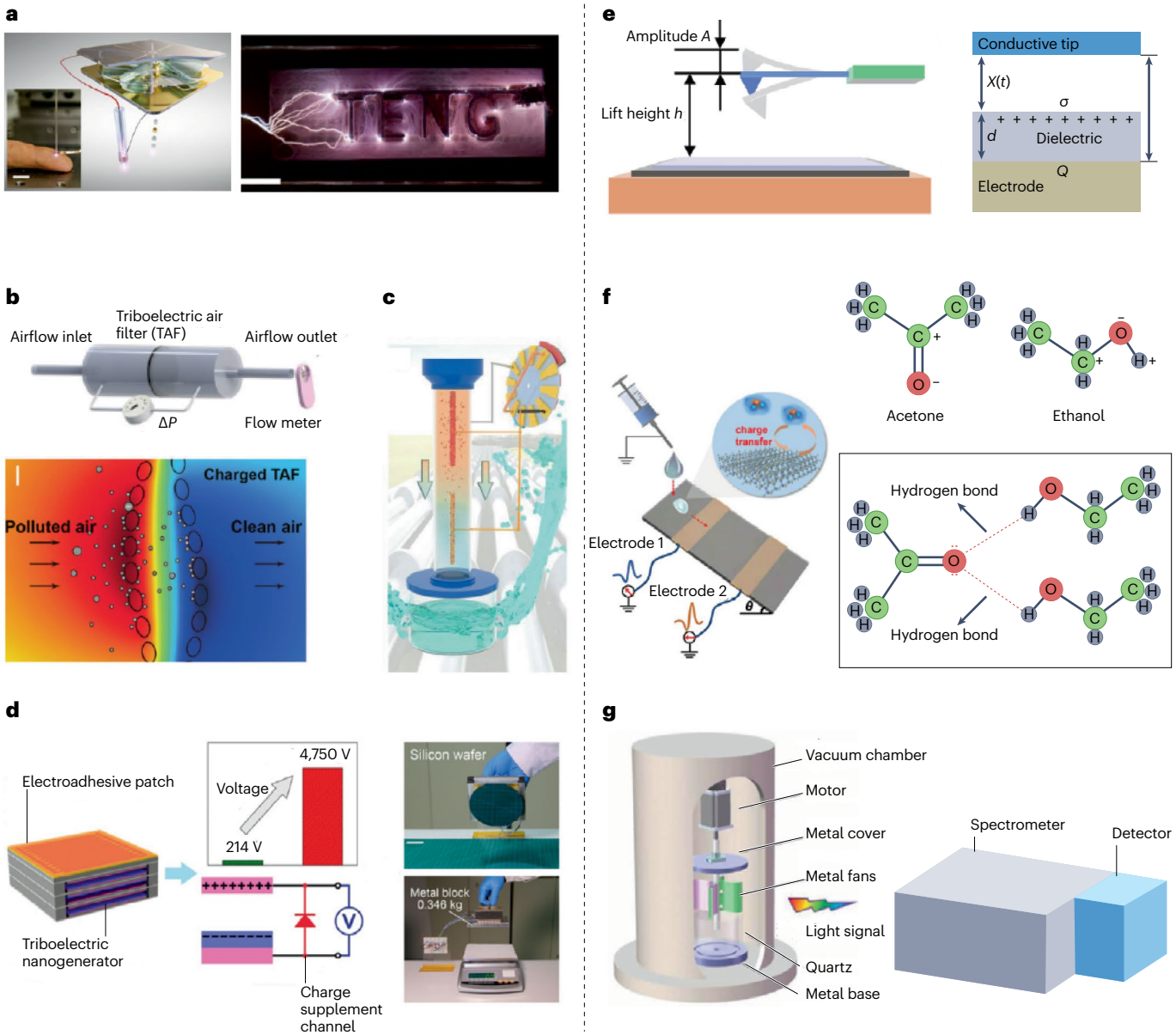


**Fig. 6 | Applications of TENGs as high-voltage power sources and probes.** **a**, An atmospheric-pressure non-equilibrium plasma jet directly driven by two serial freestanding rotary triboelectric nanogenerators (TENGs). **b**, Set-up for the measurement of the flow rate, pressure drop and particulate matter removal efficiency. **c**, TENG for an oil purification system and its practical effect demonstration. **d**, The self-powered electroadhesion system of a TENG. **e**, Set-up of the scanning TENG for solid–solid interface monitoring. **f**, The scanning TENG for solid–liquid interface monitoring. **g**, The application of a TENG for interface spectroscopy. Part **a** reprinted from ref. 56, Springer Nature Limited. Part **b** reprinted with permission from ref. 13, Wiley. Part **c** reprinted with permission from ref. 75, RSC. Part **d** reprinted with permission from ref. 76. Copyright 2018 American Chemical Society. Part **e** reprinted from ref. 14, with the permission 27 Feb 23, 4:46 PM RightsLink Printable License https://s100.copyright.com/AppDispatchServlet 3/3 of AIP Publishing. Part **f** reprinted with permission from ref. 15. Copyright 2021 American Chemical Society. Part **g** reprinted with permission from ref. 77, AAAS.

software, MATLAB (Mathworks Inc.) and C/C++. After solving the governing equation, the transient and steady-state output of TENGs can be predicted systematically. With the same charge distributions and boundary conditions, similar results are obtained regardless of the calculation method used.

## Limitations and optimizations

Although there has been progress in the basic science and applications of TENGs, limitations and challenges remain, including improvements to surface charge density, current output, humidity resistance, durability, stability and packaging technology.

Future research aimed at specific applications, such as blue energy, requires further studies of the method and mechanism, in addition to analysis of materials selection and structural design. Surface charge density is critical to TENG performance. Therefore, the material surface engineering should be given more attention to achieve high performance, focused not only on the contact separation mode but also on other TENG modes. Various microstructures and nanostructures applied in triboelectric materials are effective at enhancing TENG output performance. However, proper surface structures are still lacking for many materials. Suitable theoretical simulations and structural observation methods are needed. Polymers and metals commonly used as triboelectric materials can improve TENG performance by surface modification. Semiconductors are another important triboelectric material that is currently unexplored. The inherent high impedance characteristics means that TENGs usually exhibit low current output with a pulse form, but most electronic devices and energy storage units — including lithium batteries and supercapacitors — require DC power. As a result, effort should focus on developing specialized power management and energy storage circuits. As an entirely novel sensing method, TENG-based self-powered sensing systems can be applied in many fields, such as the Internet of Things, intelligent equipment, robotics, infrastructure monitoring, environmental monitoring, wearable devices and health care. For improved practical applications, some characteristics — in particular, high sensing accuracy, high durability and stability — should be further investigated. TENGs are a revolutionary technology for environmental micro/nano-energy harvesting and self-powered sensors and systems, especially blue energy harvesting. The influence of the service environment means performance degradation of TENGs is inevitable. Reliable packaging technology is necessary to reduce the effects of humidity, corrosion and other factors in harsh environments.

## Outlook

### TENG fundamentals and applications

This Primer has focused on the physical fundamentals, advanced technologies and applications of TENGs. To understand how the triboelectric charges are created, how the electrical charges flow and how the electric current is used for advanced technologies, a multidisciplinary approach was required, linking physics, mathematics, chemistry, engineering, material science and computer science. By examining these aspects of TENGs, new questions have arisen, which require further theoretical and experimental studies in future work.

By coupling contact electrification and electrostatic induction, a TENG device can convert mechanical energy into electric power or signal. The displacement current acts as the driving force to harvest energy from the external environment. To describe the mechanism of contact electrification, the Wang transition model is proposed, where electron transition occurs generally between any two materials or phases, including solid–solid, liquid–solid, liquid–liquid, gas–solid and gas–liquid interactions. If an electron transition exists between two dielectric surfaces, a relevant TENG device could be designed; however, this is only a theoretical possibility.

A novel term of mechano-induced polarization $\boldsymbol{P_s}$ has been added to the displacement vector. This requires generalization of constitutive relations, resulting in a modification of Maxwell's equations. Taking the expanded Maxwell's equations as the physical principle, the mathematical-physical model of TENGs can be built. Following this, the equivalent circuit model, including the capacitor model and Norton's equivalent circuit model, is established and can be constructed from the theory of lumped-parameter equivalent circuit. The lumped parameter circuit is a new, user-friendly abstraction layer created on top of Maxwell's equations, implying a high application value for electric engineering. Applications of TENGs have largely focused on the following areas: micro/nano-power sources, self-powered sensors, blue energy harvesters, high-voltage sources and as a scanning probe for liquid–solid interface charge transfer.

## Glossary

**Blue energy**
The energy captured by triboelectric nanogenerators for harvesting low-frequency water wave energy from the ocean.

**Contact electrification**
A scientific effect, primarily through the electron transfer mechanism, where two or more different materials become electrically charged after being separated from physical contact.

**Electrostatic induction**
A modification to the distribution of electric charge on one material caused by the influence of nearby materials that have electric charge.

**Energy harvesting devices**
Devices that typically produce a small amount of energy through a process that harvests energy from external sources.

**Lorentz covariance**
An equivalence of observation, as special relativity implies that the laws of physics are the same for all observers moving with respect to one another within an inertial frame.

**Lumped-parameter equivalent circuit**
A theoretical circuit that retains all the electrical characteristics of a given circuit, generally built based on a lumped parameter (or lumped element) model.

**Mechano-induced polarization**
Polarization due to pre-existing electrostatic charges and medium movement driven by external mechanical action.

**Triboelectrification**
A united process of tribology and interfacial charge transfer, one of the fundamental effects in electricity generation.

### Method of contact electrification

In practice, contact electrification involves a surprising number of scientific disciplines. Except for technology-based TENGs, at least four closely related areas have been created and their developments rely on the context in which they are applied. The first is the Wang model for the EDL[20,83], which revealed that formation of the EDL requires two steps: electron exchange between liquid and solid surfaces due to contact electrification, which makes atoms on the solid surface ions; and interaction of ions with ions in the liquid, resulting in a gradient distribution of cations and anions near the interface[3,20]. This is different to the traditional understanding of the EDL, which ignores the first step. The second field created by TENGs is contact electrification-induced interface spectroscopy[77,78], which was recently discovered and has not yet received enough attention. Electron transfer occurs from one atom in one material to another atom of another material, leading to photon emission. It was recently proved theoretically that some unstable excited electrons at a higher energy level of one material may transit to a lower energy state, resulting in contact electrification-induced interface photon spectroscopy. Confirming the physical process during contact electrification will give a better understanding of how dielectric materials act as the charge behind contact electrification.

When contact electrification occurs at an FEP–water interface, electron exchange at the interface can directly catalyse reactions without the need for conventional catalysts. Through a combination of contact electrification, mechanochemistry and catalysis, contact electrocatalysis is proposed[79]. This could expand the range of catalytic materials and provide an effective approach for exploring catalytic processes with mechano-induced contact electrification. If a semiconductor material is used in contact electrification — for example to form a metal/semiconductor[84], metal/insulator/semiconductor[85], liquid/semiconductor[86] or p-type/n-type junction system[87] — a DC can be created under external mechanical excitation. This phenomenon is known as the tribovoltaic effect[88]. Originating from this effect, several multiphysics phenomena have arisen, including the tribovoltaic-thermoelectric effect[89] and the tribo-photovoltaic effect, which was observed in dynamic metal/semiconductor Schottky systems[90].

## Emerging potential areas

Electromagnetics has had a tremendous impact on science and technology. Despite its age, electromagnetics continues to be studied due to the importance of Maxwell's equations. The TENG-based energy harvesting system is just one example of a new technology application. Although development of the MEs-f-MDMS was driven by experimental progress of TENGs, their influence is not limited to energy conversion. Several emerging potential areas directly impacted by MEs-f-MDMS include wireless communication and propagation, antenna, small antenna analysis and design, Radar, radar cross-section analysis and design, electromagnetic compatibility and electromagnetic interference analysis and design, optical imaging and optoelectronics, quantum optics and quantum information. Engineering techniques and real-world applications driven by MEs-f-MDMS focus on nanogenerators, self-powered systems and self-charging power units, which are receiving extensive attention. With wisdom, cooperation and hard work, significant word problems can be addressed, including the energy crisis and environmental pollution, to develop advanced science and technologies for the future.

Published online: 18 May 2023

## References


1. Fan, F. et al. Flexible triboelectric generator. *Nano Energy* **1**, 328–334 (2012).
   **To our knowledge, this paper is the first about the triboelectric generator, which can convert mechanical energy into electricity in the energy harvesting field.**
2. Wang, Z. L. From contact-electrification to triboelectric nanogenerators. *Rep. Prog. Phys.* **84**, 096502 (2021).
   **This paper presents a comprehensive summary of the fundamental science and working mechanism as well as important experiments of TENGs.**
3. Wang, Z. L. Triboelectric nanogenerator (TENG) — sparking an energy and sensor revolution. *Adv. Energy Mater.* **10**, 2000137 (2020).
4. Wang, Z. L. et al. *Triboelectric Nanogenerators* (Springer, 2016).
5. Shao, J., Willatzen, M. & Wang, Z. L. Theoretical modelling of triboelectric nanogenerators (TENGs). *J. Appl. Phys.* **128**, 111101 (2020).
6. Cheng, G., Lin, Z., Du, Z. & Wang, Z. L. Simultaneously harvesting electrostatic and mechanical energies from flowing water by a hybridized triboelectric nanogenerator. *ACS Nano* **8**, 1932–1939 (2014).
7. Guo, H. et al. A water-proof triboelectric–electromagnetic hybrid generator for energy harvesting in harsh environments. *Adv. Energy Mater.* **6**, 1501593 (2016).
8. Yang, J. et al. Triboelectrification-based organic film nanogenerator for acoustic energy harvesting and self-powered active acoustic sensing. *ACS Nano* **8**, 2649–2657 (2014).
9. Yang, P. et al. Paper-based origami triboelectric nanogenerators and self-powered pressure sensors. *ACS Nano* **9**, 901–907 (2015).
   **This paper is a selected representative work about TENGs, which can be used as self-powered sensors for characterizing mechanical triggers under external mechanical triggering.**
10. Xu, L. et al. Coupled triboelectric nanogenerator networks for efficient water wave energy harvesting. *ACS Nano* **12**, 1849–1858 (2018).
11. Liu, L. et al. Nodding duck structure multi-track directional freestanding triboelectric nanogenerator toward low-frequency ocean wave energy harvesting. *ACS Nano* **15**, 9412–9421 (2021).
12. Cheng, J. et al. Triboelectric microplasma powered by mechanical stimuli. *Nat. Commun* **9**, 3733 (2018).
    **This work introduces a typical characteristic of TENGs, their high output voltage.**
13. Bai, Y. et al. Washable multilayer triboelectric air filter for efficient particulate matter PM2.5 removal. *Adv. Funct. Mater.* **28**, 1706680 (2018).
14. Lin, S. & Wang, Z. L. Scanning triboelectric nanogenerator as a nanoscale probe for measuring local surface charge density on a dielectric film. *Appl. Phys. Lett.* **118**, 193901 (2021).
15. Zhang, J., Lin, S., Zheng, M. & Wang, Z. L. Triboelectric nanogenerator as a probe for measuring the charge transfer between liquid and solid surfaces. *ACS Nano* **15**, 14830–14837 (2021).
    **This work verifies that a single-electrode TENG can be a probe for measuring the charge transfer at a liquid–solid interface.**
16. Dharmasena, R. D. I. G. et al. Triboelectric nanogenerators: providing a fundamental framework. *Energy Environ. Sci.* **10**, 1801 (2017).
17. Dharmasena, R. D. et al. Nature of power generation and output optimization criteria for triboelectric nanogenerators. *Adv. Energy Mater.* **8**, 1802190 (2018).
18. Shao, J., Willatzen, M., Shi, Y. & Wang, Z. L. 3D mathematical model of contact-separation and single-electrode mode triboelectric nanogenerators. *Nano Energy* **60**, 630–640 (2019).
    **To our knowledge, this paper establishes the first 3D mathematical model based on Maxwell's equations of TENGs.**
19. Shao, J., Liu, D., Willatzen, M. & Wang, Z. L. Three-dimensional modeling of alternating current triboelectric nanogenerator in the linear sliding mode. *Appl. Phys. Rev.* **7**, 011405 (2020).
20. Wang, Z. L. et al. On the origin of contact-electrification. *Mater. Today* **30**, 34–51 (2019).
21. Shao, J. et al. Designing rules and optimization of triboelectric nanogenerator arrays. *Adv. Energy Mater.* **11**, 2100065 (2021).
    **This paper presents universal design rules and holistic optimization strategies for the network structure of TENGs, which is used as micro and nano-power sources.**
22. Shao, J. et al. Structural figure-of-merits of triboelectric nanogenerators at powering loads. *Nano Energy* **51**, 688 (2018).
23. Shao, J., Jiang, T. & Wang, Z. L. Theoretical foundations of triboelectric nanogenerators (TENGs). *Sci. China. Technol. Sci.* **63**, 1087–1109 (2020).
24. Guo, X. et al. Three-dimensional mathematical modelling and dynamic analysis of freestanding triboelectric nanogenerators. *J. Phys. D Appl. Phys.* **55**, 345501 (2022).
25. Guo, X. et al. Theoretical model and optimal output of a cylindrical triboelectric nanogenerator. *Nano Energy* **92**, 106762 (2022).
26. Guo, X. et al. Quantifying output power and dynamic charge distribution in sliding mode freestanding triboelectric nanogenerator. *Adv. Phys. Res.* https://doi.org/10.1002/apxr.202200039 (2022).
27. Wang, Z. L. Maxwell's equations for a mechano-driven, shape-deformable, charged media system, slowly moving at an arbitrary velocity field $\boldsymbol{v}(\boldsymbol{r}, t)$. *J. Phys. Commun.* **6**, 085013 (2022).
28. Wang, Z. L. The expanded Maxwell's equations for a mechano-driven media system that moves with acceleration. *Intern. J. Mod. Phys. B* https://doi.org/10.1142/S021797922350159X (2022).
29. Wang, Z. L. & Shao, J. Maxwell's equations for a mechano-driven varying-speed motion media system under slow motion and nonrelativistic approximations [Chinese]. *Sci. Sin. Tech.* **52**, 1198–1211 (2022).
30. Wang, Z. L. & Shao, J. Maxwell's equations for a mechano-driven varying-speed-motion media system for engineering electrodynamics and their solutions [Chinese]. *Sci. Sin. Tech.* **52**, 1416–1433 (2022).
31. Wang, Z. L. & Shao, J. From Faraday's law to the expanded Maxwell's equations for a mechano-driven media system that moves with acceleration [Chinese]. *Sci. Sin. Tech.* https://doi.org/10.1360/SST-2022-0322 (2022).
32. Wang, Z. L. On the first principle theory of nanogenerators from Maxwell's equations. *Nano Energy* **68**, 104272 (2020).
    **To our knowledge, this work presents the first principle theory of TENGs from Maxwell's equations.**
33. Wang, Z. L. On the expanded Maxwell's equations for moving charged media system — general theory, mathematical solutions and applications in TENG. *Mater. Today* **52**, 348–363 (2021).
34. Wang, H. et al. A paradigm-shift fully-self-powered long-distance wireless sensing solution enabled by discharge induced displacement current. *Sci. Adv.* **7**, eabi6751 (2021).
35. Cao, X. et al. An easy and efficient power generator with ultrahigh voltage for lighting, charging and self-powered systems. *Nano Energy* **100**, 107409 (2022).
36. Zhao, H. et al. Underwater wireless communication via TENG-generated Maxwell's displacement current. *Nat. Commun.* **13**, 3325 (2022).
37. Shao, J. et al. Quantifying the power output and structural figure-of-merits of triboelectric nanogenerators in a charging system starting from the Maxwell's displacement current. *Nano Energy* **59**, 380–389 (2019).
38. Niu, S. et al. Theoretical study of contact-mode triboelectric nanogenerators as an effective power source. *Energy Environ. Sci.* **6**, 3576 (2013).
    **To our knowledge, this work proposes the first equivalent circuit model of TENGs.**

39. Niu, S. et al. Theoretical investigation and structural optimization of single-electrode triboelectric nanogenerators. *Adv. Funct.Mater.* **24**, 3332–3340 (2014).
40. Niu, S. et al. Theory of sliding-mode triboelectric nanogenerators. *Adv.Mater.* **25**, 6184–6193 (2013).
41. Niu, S. et al. Theory of freestanding triboelectric-layer-based nanogenerators. *Nano Energy* **12**, 760–774 (2015).
42. Jiang, T. et al. Figures-of-merit for rolling-friction-based triboelectric nanogenerators. *Adv. Mater. Technol.* **1**, 1600017 (2016).
43. Chen, B. et al. Water wave energy harvesting and self-powered liquid-surface fluctuation sensing based on bionic-jellyfish triboelectric nanogenerator. *Mater. Today* **21**, 88–97 (2018).
44. Niu, S. & Wang, Z. L. Theoretical systems of triboelectric nanogenerators. *Nano Energy* **14**, 161 (2015).
45. Peng, J., Kang, S. D. & Snyder, G. J. Optimization principles and the figure of merit for triboelectric generators. *Sci. Adv.* **3**, eaap8576 (2017).
46. Zi, Y. L. et al. Standards and figure-of-merits for quantifying the performance of triboelectric nanogenerators. *Nat. Commun.* **6**, 8376 (2015).
47. Li, X. et al. Stimulation of ambient energy generated electric field on crop plant growth. *Nat. Food* **3**, 133–142 (2022).
48. Rana, S. M. S. et al. Ultrahigh-output triboelectric and electromagnetic hybrid generator for self-powered smart electronics and biomedical applications. *Adv. Energy Mater.* **12**, 2202238 (2022).
49. Chen, P. et al. Achieving high power density and durability of sliding mode triboelectric nanogenerator by double charge supplement strategy. *Adv. Energy Mater.* **12**, 2201813 (2022).
50. Zhang, X. et al. Broadband vibration energy powered autonomous wireless frequency monitoring system based on triboelectric nanogenerators. *Nano Energy* **98**, 107209 (2022).
51. Guo, Y. et al. Multifunctional mechanical sensing electronic device based on triboelectric anisotropic crumpled nanofibrous mats. *ACS Appl. Mater. Interfaces* **13**, 55481–55488 (2021).
52. Zhang, D. et al. Multi-grating triboelectric nanogenerator for harvesting low-frequency ocean wave energy. *Nano Energy* **61**, 132–140 (2019).
53. Guo, H. et al. An ultrarobust high-performance triboelectric nanogenerator based on charge replenishment. *ACS Nano* **9**, 5577–5584 (2015).
54. Lin, Z. et al. Super-robust and frequency-multiplied triboelectric nanogenerator for efficient harvesting water and wind energy. *Nano Energy* **64**, 103908 (2019).
55. Yang, J. et al. Broadband vibrational energy harvesting based on a triboelectric nanogenerator. *Adv. Energy Mater.* **4**, 1301322 (2014).
56. Liang, X. et al. Spherical triboelectric nanogenerator integrated with power management module for harvesting multidirectional water wave energy. *Energy Environ. Sci.* **13**, 277–285 (2020).
57. Han, J. et al. Energy autonomous paper modules and functional circuits. *Energy Environ. Sci.* **15**, 5069 (2022).
58. Zi, Y. et al. Effective energy storage from a triboelectric nanogenerator. *Nat. Commun.* **7**, 10987 (2016).
59. Ren, Z. et al. Water-wave driven route avoidance warning system for wireless ocean navigation. *Adv. Energy Mater.* **11**, 2101116 (2021).
60. Cheng, R. et al. Enhanced output of on-body direct-current power textiles by efficient energy management for sustainable working of mobile electronics. *Adv. Energy Mater.* **12**, 2201532 (2022).
61. Liang, X., Liu, S., Ren, Z., Jiang, T. & Wang, Z. L. Self-powered intelligent buoy based on triboelectric nanogenerator for water level alarming. *Adv. Funct. Mater.* **32**, 2205313 (2022).
62. Xi, F. et al. Self-powered intelligent buoy system by water wave energy for sustainable and autonomous wireless sensing and data transmission. *Nano Energy* **61**, 1–9 (2019).
63. Zhang, X. et al. Harvesting multidirectional breeze energy and self-powered intelligent fire detection systems based on triboelectric nanogenerator and fluid-dynamic modeling. *Adv. Funct. Mater*. **31**, 2106527 (2021).
64. Li, C. et al. Sensing of joint and spinal bending or stretching via a retractable and wearable badge reel. *Nat. Commun.* **12**, 2950 (2021).
65. Yang, J. et al. 3D-printed bearing structural triboelectric nanogenerator for intelligent vehicle monitoring. *Cell Rep. Phys. Sci.* **2**, 100666 (2021).
66. Wang, Z. et al. A self-powered angle sensor at nanoradian-resolution for robotic arms and personalized medicare. *Adv. Mater.* **13**, 2001466 (2020).
67. Peng, X. et al. All-nanofiber self-powered skin-interfaced real-time respiratory monitoring system for obstructive sleep apnea-hypopnea syndrome diagnosing. *Adv. Funct. Mater.* **20**, 2103559 (2021).
68. Wang, Z. L. Triboelectric nanogenerators as new energy technology and self-powered sensors — principles, problems and perspectives. *Faraday Discuss* **176**, 447–485 (2014).
69. Wang, Z. L. Nanogenerators, self-powered systems, blue energy, piezotronics and piezophototronics — a recall on the original thoughts for coining these fields. *Nano Energy* **54**, 477–483 (2018).
70. Wang, Z. L. Catch wave power in floating nets. *Nature* **542**, 159–160 (2017).
71. Yang, X. et al. Macroscopic self-assembly network of encapsulated high-performance triboelectric nanogenerators for water wave energy harvesting. *Nano Energy* **60**, 404–412 (2019).
72. Wang, H., Xu, L., Bai, Y. & Wang, Z. L. Pumping up the charge density of a triboelectric nanogenerator by charge-shuttling. *Nat. Commun.* **11**, 4203 (2020).
73. Jiang, T. et al. Robust swing-structured triboelectric nanogenerator for efficient blue energy harvesting. *Adv. Energy Mater.* **10**, 2000064 (2020).
74. Wang, Z. L., Jiang, T. & Xu, L. Toward the blue energy dream by triboelectric nanogenerator networks. *Nano Energy* **39**, 9–23 (2017).
**This paper introduces one of the important uses of TENGs to harvest energy from the ocean or wave energy.**
75. Lei, R. et al. Sustainable high-voltage source based on triboelectric nanogenerator with a charge accumulation strategy. *Energy Environ. Sci* **13**, 2178–2190 (2020).
76. Xu, L. et al. Giant voltage enhancement via triboelectric charge supplement channel for self-powered electroadhesion. *ACS Nano* **12**, 10262–10271 (2018).
77. Li, D. et al. Interface inter-atomic electron-transition induced photon emission in contact-electrification. *Sci. Adv.* **7**, eabj0349 (2021).
78. Nan, Y. et al. Physical mechanisms of contact-electrification induced photon emission spectroscopy from interfaces. *Nano Res.* https://doi.org/10.1007/s12274-023-5674-2 (2023).
79. Wang, Z. et al. Contact-electro-catalysis for the degradation of organic pollutants using pristine dielectric powders. *Nat. Commun.* **13**, 130 (2022).
80. Zou, H. et al. Quantifying the triboelectric series. *Nat. Commun.* **10**, 1427 (2019).
81. Zou, H. et al. Quantifying and understanding the triboelectric series of inorganic non-metallic materials. *Nat. Commun.* **11**, 2093 (2020).
82. Wang, Z. L., Chen, J. & Lin, L. Progress in triboelectric nanogenerators as new energy technology and self-powered sensors. *Energy Environ. Sci.* **8**, 2250 (2015).
83. Lin, S., Chen, X. & Wang, Z. L. Contact electrification at the liquid–solid interface. *Chem. Rev.* **122**, 5209–5232 (2022).
84. Liu, J. et al. Direct-current triboelectricity generation by a sliding schottky nanocontact on $MoS_2$ multilayers. *Nat. Nanotechnol* **13**, 112–116 (2018).
85. Hao, Z. et al. Co-harvesting light and mechanical energy based on dynamic metal/perovskite Schottky junction. *Matter* **1**, 639–649 (2019).
86. Lin, S., Chen, X. & Wang, Z. L. The tribovoltaic effect and electron transfer at a liquid–semiconductor interface. *Nano Energy* **76**, 105070 (2020).
87. Xu, R. et al. Direct current triboelectric cell by sliding an n-type semiconductor on a p-type semiconductor. *Nano Energy* **66**, 104185 (2019).
88. Zhang, Z. et al. Tribovoltaic effect on metal–semiconductor interface for direct-current low-impedance triboelectric nanogenerators. *Adv. Energy Mater.* **10**, 1903713 (2020).
89. Zhang, Z. et al. Tribo-thermoelectric and tribovoltaic coupling effect at metal–semiconductor interface. *Mater. Today Phys.* **16**, 100295 (2021).
90. Zheng, M. et al. Photovoltaic effect and tribovoltaic effect at liquid–semiconductor interface. *Nano Energy* **83**, 105810 (2021).


## Acknowledgements

T.H.C. and J.J.S. contributed equally to this work. The authors are grateful for the support from the National Key R&D Project from the Minister of Science and Technology (Nos. 2021YFA1201601 and 2021YFA1201604), the National Natural Science Foundation of China (Grant Nos. 62001031) and the Youth Innovation Promotion Association, CAS.

## Author contributions

Introduction (J.J.S. and Z.L.W.); Experimentation (T.H.C. and J.J.S.); Results (J.J.S. and Z.L.W.); Applications (T.H.C. and Z.L.W.); Reproducibility and data deposition (J.J.S.); Limitations and optimizations (T.H.C.); Outlook (J.J.S. and Z.L.W.); Overview of the Primer (Z.L.W.).

## Competing interests

The authors declare no competing interests.

## Additional information

**Peer review information** *Nature Reviews Methods Primers* thanks Jeffrey Snyder and the other, anonymous, reviewer(s) for their contribution to the peer review of this work.

**Publisher's note** Springer Nature remains neutral with regard to jurisdictional claims in published maps and institutional affiliations.